SLAC-PUB-9374
August 2002

# SUBMICRON X-RAY DIFFRACTION AND ITS APPLICATIONS TO PROBLEMS IN MATERIALS AND ENVIRONMENTAL SCIENCE

**N. Tamura[1], R. Spolenak[2], B.C. Valek[3], A. Manceau[4], N. Meier Chang[3], R.S. Celestre[1], A.A. MacDowell[1], H.A. Padmore[1], & J.R. Patel[1,5]**

[1] *ALS/LBL,1 Cyclotron Road, Berkeley, CA 94720, USA*

[2] *Agere Systems, formerly of Bell Labs, Lucent Technologies, Murray Hill, NJ 07974, USA*

[3] *Dept. of Mat. Sci. & Eng., Stanford University, Stanford, CA 94305, USA*

[4] *Environmental Geochemistry Group, LGIT, University J. Fourier, 38041 Grenoble Cedex 9, France*

[5] *SSRL/SLAC, Stanford University, Stanford, CA 94309, USA*

## Abstract

The availability of high brilliance 3rd generation synchrotron sources together with progress in achromatic focusing optics allow to add submicron spatial resolution to the conventional century-old X-ray diffraction technique. The new capabilities include the possibility to map *in-situ*, grain orientations, crystalline phase distribution and full strain/stress tensors at a very local level, by combining white and monochromatic X-ray microbeam diffraction. This is particularly relevant for high technology industry where the understanding of material properties at a microstructural level becomes increasingly important. After describing the latest advances in the submicron X-ray diffraction techniques at the ALS, we will give some examples of its application in material science for the measurement of strain/stress in metallic

Work supported in part by the Department of Energy contract DE-AC03-76SF00515.

thin films and interconnects. Its use in the field of environmental science will also be discussed.

**Keywords**

X-ray micro-diffraction, thin films, microtexture, strain/stress

---

Contact Author Nobumichi Tamura, Lawrence Berkeley National Lab., MS 2-400, Berkeley, CA 94720, tel. (510) 486 6189, fax (510) 486 7696 e-mail: ntamura@lbl.gov

## Introduction

Materials properties such as strengthening, resistance to fatigue and failure intimately depend on their microstructural features such as grains, grain boundaries, inclusions, voids and other defects. However, at the so-called mesoscopic length scale (approximately between 0.1 and 10 microns) materials typically exhibit high inhomogeneity, and properties are extremely difficult to study both experimentally and theoretically. This length scale is situated between the atomic scale of atoms and individual dislocations, and the macroscopic scale of continuum mechanics.

X-ray diffraction is a powerful technique, used for almost a century to measure grain orientation and strain, as well as for crystalline phase identification and structure refinement. Compared to electron microscopy, X-rays have the advantages of higher penetration depth (rendering possible the scanning of bulk and buried samples), do not require any particular sample preparation and can be used under a variety of different conditions (in air, liquid,

vacuum or gas, at different temperature and pressures). Its main drawback for the study of materials at the micron scale was until recently its poor spatial resolution.

Today, the availability of high brilliance third generation synchrotron sources, combined with progress in X-ray focusing optics and fast 2D large area detector technology have made possible the development of Scanning X-ray Microdiffraction (μSXRD) techniques using either monochromatic or polychromatic focused beams of sizes ranging from a few microns to submicron [1-8]. The closest equivalents in the electron microscopy field are STEM (Scanning Transmission Electron Microscopy) and EBSD (Electron Back Scatter Diffraction). The spatial resolution of electron microscopy is still about an order of magnitude better than focused X-rays, but the two techniques are complementary, with X-ray microdiffraction being a superior technique for looking at sub-surface structures, and for precision measurements of stress.

Recently, an X-ray microdiffraction end station capable of measuring grain orientation and triaxial strain in arbitrarily oriented micron-sized crystals became available at the Advanced Light Source on beamline 7.3.3. This paper describes practical applications provided by this tool.

**Beamline Description**

The experimental setting of the 7.3.3. beamline end station is shown in Fig. 1 and has been described in details elsewhere [8]. The X-ray synchrotron beam from a bending magnet source is focused via a pair of bendable Kirkpatrick-Baez mirrors to a submicron size (0.7x0.8 μm FWHM). A 4-crystal Si (111) monochromator is used to easily switch between white and monochromatic beams while the same area on the sample is illuminated. The sample is

usually in the reflective geometry arrangement, the surface making an angle of 45° relatively to the incoming beam. The outgoing Bragg reflections are collected using a large area CCD detector (Bruker 6000, active area of 9x9 cm) placed ~ 3 cm above the sample. For single crystals and polycrystalline samples with grain size of the order of a micron, the so-called white beam or Laue reflection technique is used. Illuminating an area of interest with submicron white beam provides a Laue pattern which can be image-treated and automatically indexed. The indexing yields at the same time the crystal orientation and deviatoric (distortional) strain tensor of the illuminated area. By putting the sample on an X-Y piezo stage, it can be scanned under the focused beam with submicron step size. This allows orientation and strain/stress mapping of the material. The complete strain tensor (6 components) can also be computed by additionally determining the dilatational ("hydrostatic") component. This can be achieved by measuring the energy of at least one reflection using the monochromator [1, 2, 4]. For finely grained samples, monochromatic beam is preferentially used and a powder ring pattern is collected at each step of the X-Y scan. A solid state detector coupled with a multichannel analyzer allows for the parallel collection of fluorescence signals which allows for elemental mapping. A software package developed at the ALS (X-MAS for X-Ray Microdiffraction Analysis Software) is used for data collection, Laue pattern indexing, strain refinement and monochromatic beam scans analysis. For polycrystals, an orientation map "smoothing" algorithm also allows for the automatic determination of grain boundaries by fitting the intensity profile of each individual crystal grain and intersecting the resulting normalized profiles.

**Applications**

*Thermal stress measurements in Al(Cu) interconnect*: The samples consist of patterned Al(0.5% wt Cu) lines (length: 30 μm, thickness: 0.7 μm, width: 4.1 and 0.7 μm) sputter deposited on a Si wafer and buried under a glass passivation layer (0.7 μm thick). As a comparison, data has been also taken on unpassivated Al(Cu) pads (blanket films).

Fig. 2 shows orientation and deviatoric stress maps on a 5x5 μm region in the pad and on the 4.1 μm and 0.7 μm wide lines. The stress in the pad appears to be biaxially tensile in average, which is consistent with macroscopic stress measurements using wafer curvature and conventional X-ray diffraction techniques. However, at a microscopic scale, stress is actually far from being homogeneous. It is triaxial rather than biaxial, with local differences reaching 60-80 MPa.

Similarly, lines displayed local variations of 60-80 MPa in stress for the 4.1 μm line and up to 140 MPa for the 0.7 μm line. As the line gets narrower, the level of stress gets higher and, on average, shifts from biaxial to triaxial. Orientation maps also show the change in the microstructure from polycrystalline in the pad and in the 4.1 μm line to "bamboo"-type for the 0.7 μm line. Temperature cycling experiments between 25°C and 345°C have been carried out on these same lines [9] and show good agreement of the average stress-temperature curves with those obtained with conventional techniques, but show a high degree of complexity on the local scale. Large intergranular and intragranular stress variations have been measured indicating that local parameters such as grain orientation, grain initial stress, grain size and type of grain boundaries play a crucial role in understanding the inhomogeneous yielding mechanisms of polycrystalline thin films. This particular example shows the ability of X-ray microdiffraction to provide quantitative data such as grain orientation, structure, and stress at

the local level in passivated interconnects, greatly improving the understanding and modeling of material mechanical properties under constraints.

*Electromigration in Damascene Cu interconnects*: Fig. 3 shows a region of a sputtered copper damascene interconnect (1.1 μm wide, passivated with nitride) that has undergone electromigration testing [10]. The bottom right inset shows a High Voltage Scanning Electron Microscope (HVSEM) image taken just after the electromigration test, near the cathode end. The metal build-up region (marked by a black circle) appears as a slightly darker zone in the electromigrated line. The corresponding orientation and resolved shear stress (calculated from the measured distortional stresses and considering the 12 gliding systems of Cu: (111) type planes in the <110> directions) maps obtained by μSXRD are displayed on the left. The grain structure has a random out-of-plane orientation and a near-bamboo structure. The indices, next to the map, indicate the approximate out-of-plane orientation of the largest grains. At the location of the local buildup region, the resolved shear stress dramatically increases to reach a maximum value of about 600 MPa. The orientation map shows that metal has accumulated at the interface of a (111) bamboo grain just before the location of a (115) twin and after a series of small randomly oriented grains (the latter will allow for a fast electromigration diffusion path). The width of the Bragg reflections also contains information on the dislocation density and provides an indication on the level of stress and plastic deformation inside a particular grain. The peak width of the (113) reflection is plotted (top right) as a function of the position along the 2 μm long (111) grain (indicated by the black double-sided arrow next to the orientation map), which contains the (115) blocking twin. The peak is clearly broader in the buildup region next to the twin boundary.

Electromigration-induced failure in interconnect metal lines are highly dependant on the microstructure and initial stress state of the samples. The capability demonstrated by the instrument to non-destructively probe local grain structure as well as stress becomes particularly relevant to the understanding of microstructure-related failure mechanisms and to predict where the line is likely to fail during service. This technologically important problem is shown to be much more complex when the line dimensions shrink to a size where microstructural local effects could no longer be neglected.

*Element speciation in soil micronodules*: Soils chemically and structurally highly heterogeneous, rendering the identification of finely dispersed mineral species difficult, if at all possible, with conventional laboratory diffractometers. Since environmental materials are heterogeneous on nanometer to micrometer length scales, the combination of synchrotron-based X-ray radiation microfluorescence (μSXRF) and μXRD techniques provides just the tool needed to make the key identification of most reactive constituents, and the uptake mechanism of associated trace elements. These new scientific opportunities will be illustrated by the sequestration mechanism of Zn and Ni in soils. Fig. 4 a) shows Mn, Fe, Zn and Ni chemical maps as determined by μSXRF. Zn and Ni are both associated with Mn but unlike Zn, Ni is not present in the entire Mn region, suggesting the presence of at least two distinct Mn species. A phyllosilicate component, an Fe oxyhydroxide, goethite (αFeOOH), and two Mn oxides (birnessite and lithiophorite), were positively identified by μXRD (Fig. 4b). The lithiophorite structure consists of mixed $MnO_2$ and $Al(OH)_3$ octahedral layers, whereas birnessite has a single $MnO_2$ layer structure in which Mn atoms are adsorbed in the interlayer space above and below vacant layer octahedral sites [11] (Fig. 4 c). The soil sample was

scanned with a 6 keV monochromatic beam, and a diffraction pattern was collected at each step. The automated analysis of the powder ring patterns yielded the mineral species distribution maps presented on Fig. 4 d). The comparison of chemical and mineral species maps indicates that Ni is exclusively associated with the lithiophorite, whereas Zn is partitioned between lithiophorite, birnessite and phyllosilicates (not shown). In future studies, the crystallographic sites of Ni and Zn in their host phases will be determined by μEXAFS [12]. The combination of these three micron-scale techniques is unprecedented and is quite powerful in advancing the scientific state-of-the-art for the remediation of contaminated sites.

**Conclusion**

Scanning X-ray microdiffraction using white and/or monochromatic beams offer a powerful tool to study material properties at the micron-scale. The white beam technique is suitable for in-situ study of microtexture and strain in single crystal and polycrystalline thin films. It was applied to study electromigration damage in microchip interconnects, as well as studying the effect of confinement during thermal cycles. The applicability of the technique was also recently demonstrated in the study of deformation in MEMS devices, composite materials, and in-situ uniaxial tensile testing of polycrystalline samples and will be addressed in forthcoming papers. Monochromatic μSXRD, coupled with μSXRF and μEXAFS, is a new and promising technique, which should develop in molecular environmental science [13]. Future work includes the use of monochromatic μSXRD for strain mapping in thin metallic films subject to spontaneous debonding from the substrate and metallic membranes under uniaxial tensile strain.

**Acknowledgements**

The Advanced Light Source is supported by the Director, Office of Science, Office of Basic Energy Sciences, Materials Sciences Division, of the U.S. Department of Energy under Contract No. DE-AC03-76SF00098 at Lawrence Berkeley National Laboratory. We thank Intel Corp. for the partial funding of the end station.

**References**

1.- J.S. Chung, N. Tamura, G.E. Ice, B.C Larson, J.D. Budai, W. Lowe, In Materials Reliability in Microelectronics IX, , Mat. Res. Soc. Symp. Proc., Edited by C.A. Volkert, A.H. Verbruggen, D. Brown, **563** (1999) 169-174

2.- N. Tamura, J.-S. Chung, G.E. Ice, B.C Larson, J.D. Budai, J.Z. Tischler, M. Yoon, E.L. Williams and W.P. Lowe, In Materials Reliability in Microelectronics IX, , Mat. Res. Soc. Symp. Proc., Edited by C.A. Volkert, A.H. Verbruggen, D. Brown, **563** (1999) 175-180.

3.- B.C. Larson, N. Tamura, J.-S. Chung, G.E. Ice, J.D. Budai, J.Z. Tischler, W. Yang, H. Weiland, W.P. Lowe, , Mat. Res. Soc. Symp. Proc., Edited by S.R. Stock, S.M. Mini, and D.L. Perry, **590** (2000) 247-252.

4.- N. Tamura, B. C. Valek, R. Spolenak, A. A. MacDowell, R. S. Celestre, H.A.Padmore, W. L. Brown, T. Marieb, J. C. Bravman, B. W. Batterman and J. R. Patel, Mat. Res. Soc.

Symp. Proc., Edited by G.S. Oehrlein, K. Maex, Y.-C. Joo, S. Ogawa and J.T. Wetzel, **612** (2000) D8.8.1-D8.8.6

5.-R. Spolenak, D.L. Barr, M.E. Gross, K. Evans-Lutherodt, W.L. Brown, N. Tamura, A.A. MacDowell, R.S. Celestre, H.A.Padmore, J.R. Patel, B.C. Valek, J.C. Bravman, P. Flinn, T. Marieb, R.R. Keller, B.W. Batterman, Mat. Res. Soc. Symp. Proc., Edited by G.S. Oehrlein, K. Maex, Y.-C. Joo, S. Ogawa and J.T. Wetzel, **612** (2000) D.10.3.1-D10.3.7.

6.- C. Riekel. C. Braenden, C. Craig, C. Ferrero, F. Heidelbach, M. Müller, Int. J. Mol. Biol. 24 (2-3), (1999) 187-195.

7.- C. Riekel, Rep. Prog. Phys. 63, (2000) 233-262

8.- A.A.MacDowell, R.S.Celestre, N.Tamura, R.Spolenak, B.C. Valek, W.L.Brown, J.C.Bravman, H.A.Padmore, B.W.Batterman& J.R.Patel, SRI Conference Proc., Berlin, Nuclear Instruments and Methods in Physics Research A (2000) in press

9.- B.C. Valek, N. Tamura, R. Spolenak, A.A. MacDowell, R.S. Celestre, H.A. Padmore, J.C. Bravman, W.L. Brown, B. W. Batterman and J. R. Patel, Mat. Res. Soc. Symp. Proc., **673** (2001) P7.7, in press

10.- B.C. Valek, N. Meier Chang, N. Tamura, R. Spolenak, R.S. Celestre, A.A. MacDowell, H.A. Padmore, J.C. Bravman, P. Flinn, and J.R. Patel, Appl. Phys. Lett., to be submitted.

11.- B. Lanson, V.A. Drits, E.J. Silvester and A. Manceau, Am. Miner. **85** (2000) 826.

12.- A. Manceau, B. Lanson, M.L. Schlegel, J.C. Hargé, M. Musso, L. Eybert-Bérard, J.L. Hazemann, D. Chateigner and G.M. Lamble, Am. J. Sci. **300**, (2000) 289.

13.- S. Hlawatsch, M. Kersten, C.D. Garbe-Schönberg, F. Lechtenberg, A. Manceau, N. Tamura, D.A. Kulik, J. Harff, E. Suess, Chem. Geol. (2001) in press.

**Figures Captions**

Fig.1 Schematic layout of the micro-diffraction end station on beamline 7.3.3. at the ALS.

Fig.2. In-plane orientation and deviatoric stress components along x, y and z for the Al(Cu) unpassivated blanket film (top), 4.1 μm wide passivated line (bottom left) and 0.7 μm wide passivated line (bottom right).

Fig.3 Grain orientation and resolved shear stress maps obtained by the Scanning X-ray Microdiffraction Laue technique. The HVSEM image (bottom right) shows a region of metal accumulation (see text).

Fig.4. a) Mn, Fe, Zn and Ni chemical maps of a soil micronodule obtained by μXRF. b) Microdiffraction patterns in selected regions of the map. c) Crystallographic structures of goethite, lithiophorite and hexagonal birnessite. d) Mineral species distribution maps for goethite, lithiophorite and hexagonal birnessite obtained by monochromatic μSXRD.

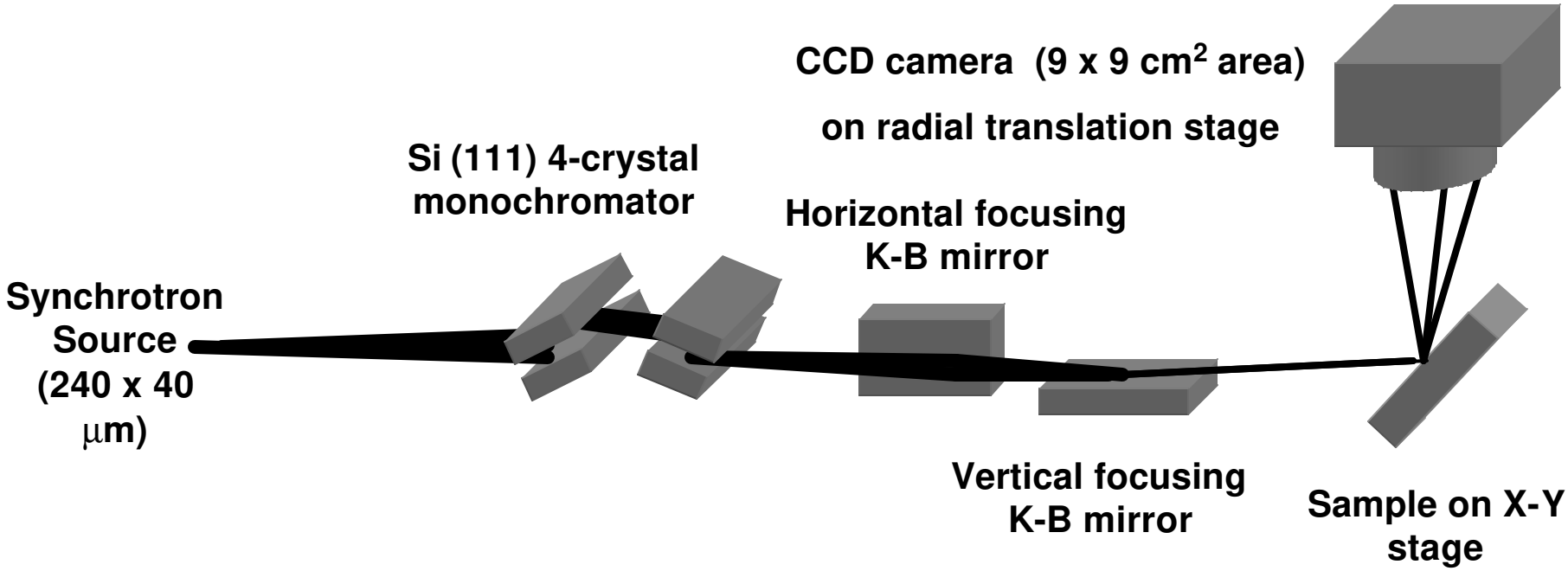
CCD camera (9 x 9 cm2 area)
on radial translation stage
Si (111) 4-crystal
monochromator
Horizontal focusing
K-B mirror
Synchrotron
Source
(240 x 40
μm)
Vertical focusing
K-B mirror
Sample on X-Y
stage

Fig. 1

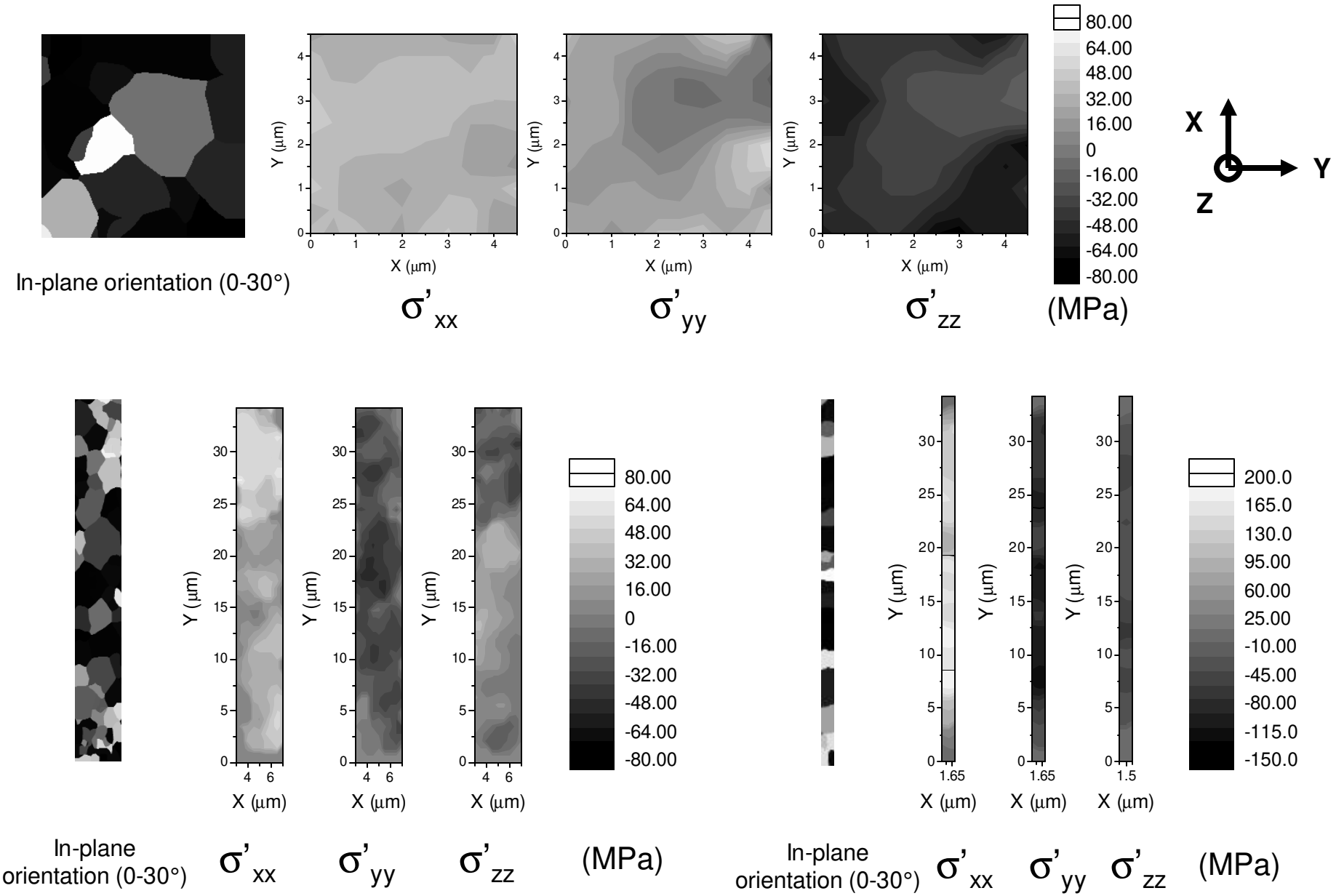
In-plane orientation (0-30°)
Y (μm)
X (μm)
σ'xx
σ'yy
σ'zz
80.00
64.00
48.00
32.00
16.00
0
-16.00
-32.00
-48.00
-64.00
-80.00
(MPa)
X
Y
Z
In-plane orientation (0-30°)
σ'xx
σ'yy
σ'zz
(MPa)
200.0
165.0
130.0
95.00
60.00
25.00
-10.00
-45.00
-80.00
-115.0
-150.0

Fig. 2

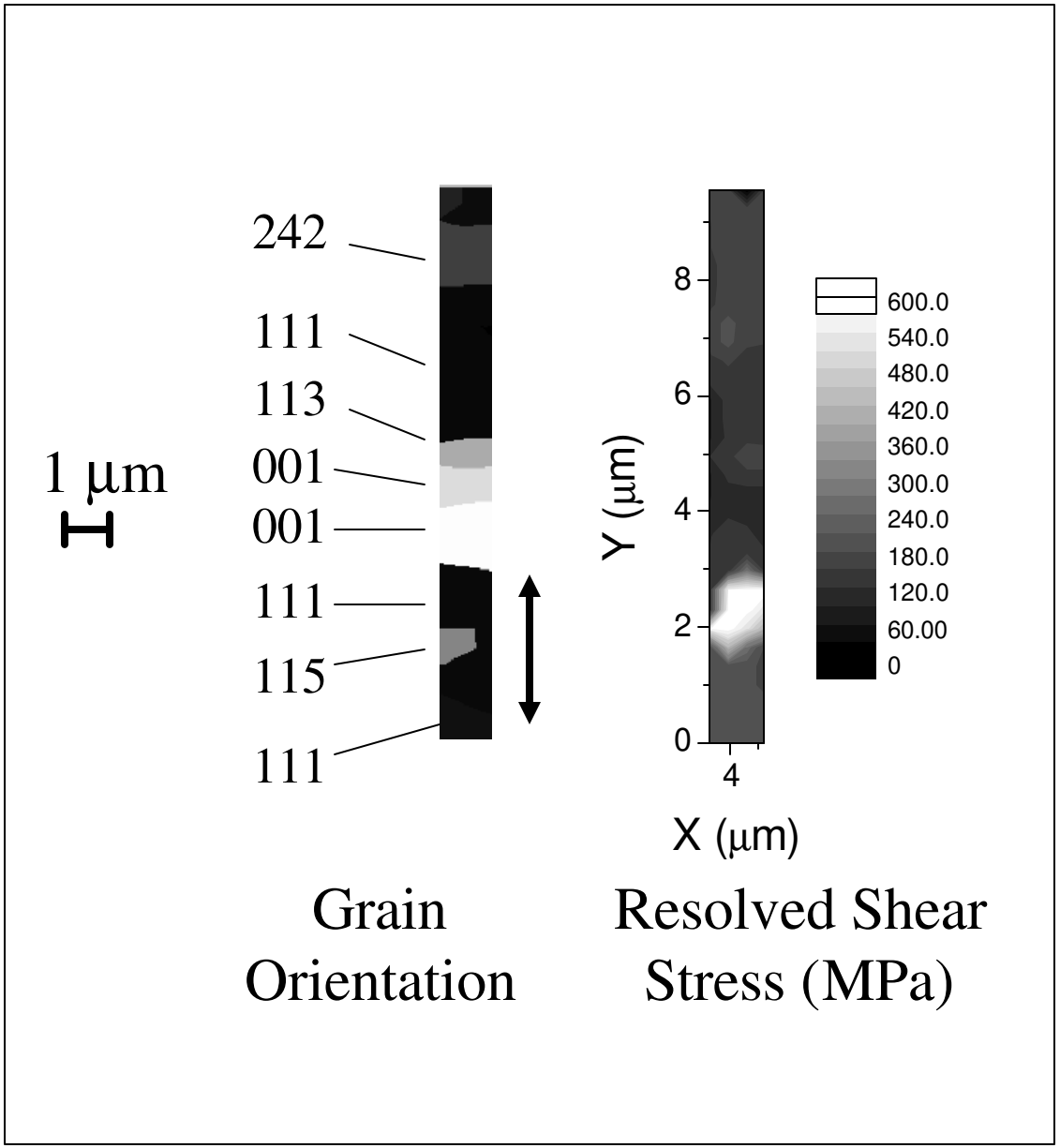
1 μm
242
111
113
001
001
111
115
111
Grain Orientation
8
6
4
2
0
Y (μm)
4
X (μm)
600.0
540.0
480.0
420.0
360.0
300.0
240.0
180.0
120.0
60.00
0
Resolved Shear Stress (MPa)

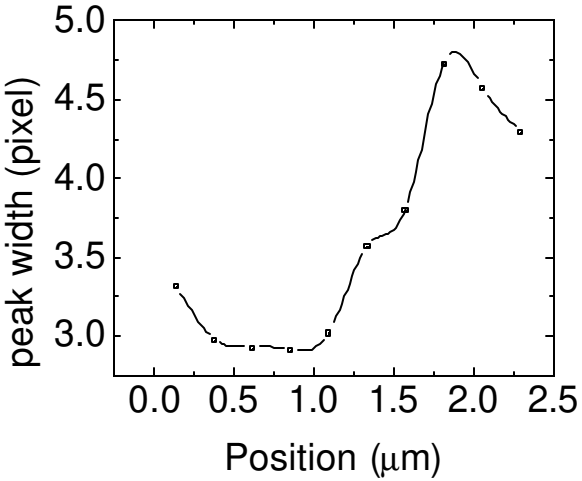
5.0
4.5
4.0
3.5
3.0
peak width (pixel)
0.0
0.5
1.0
1.5
2.0
2.5
Position (μm)

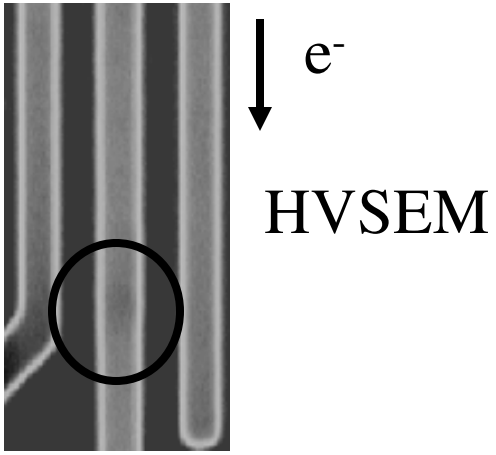
e-
HVSEM

Fig. 3

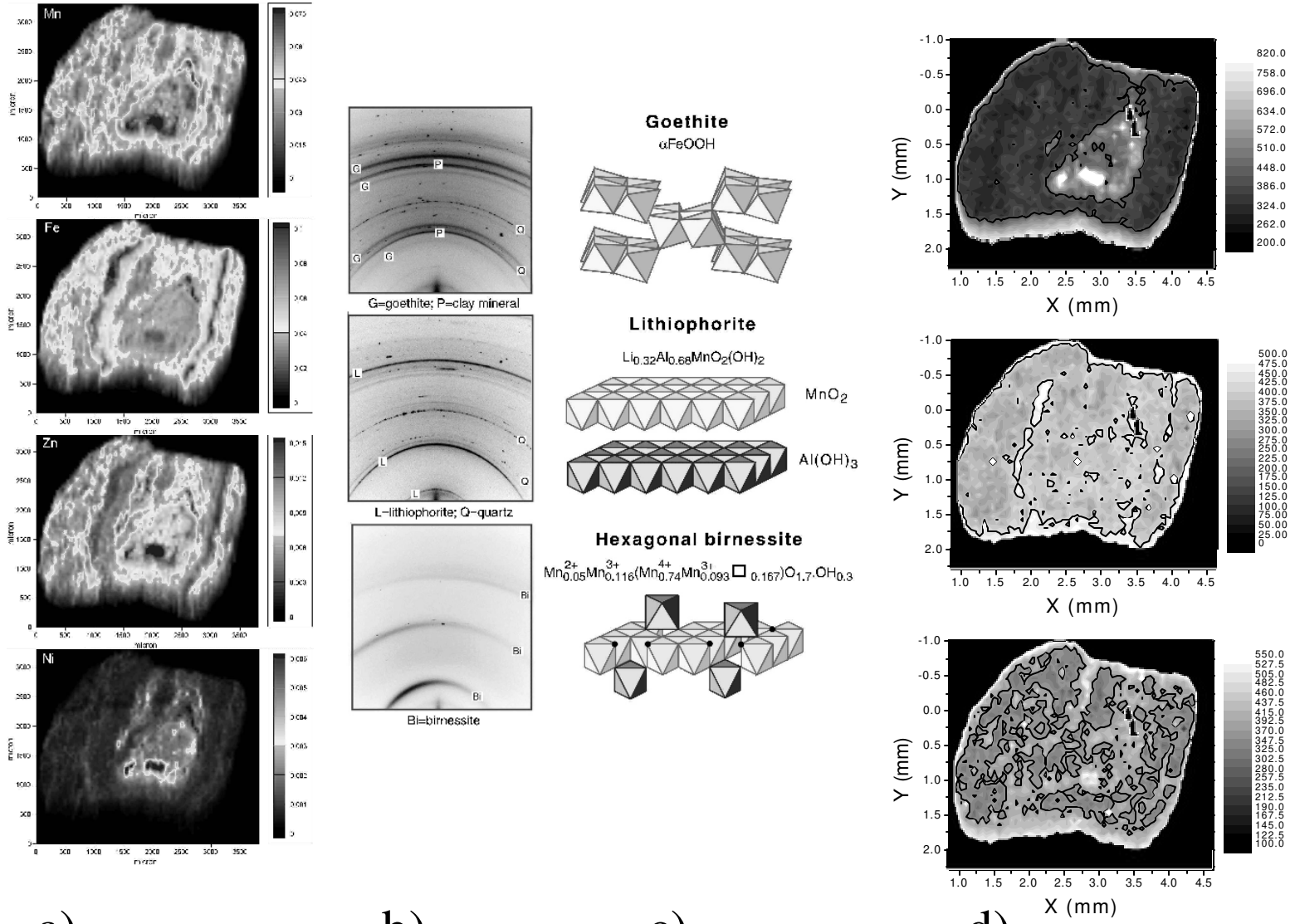
Mn
Fe
Zn
Ni
G=goethite; P=clay mineral
L=lithiophorite; Q=quartz
Bi=birnessite
Goethite
αFeOOH
Lithiophorite
Li0.32Al0.68MnO2(OH)2
MnO2
Al(OH)3
Hexagonal birnessite
Mn0.05Mn0.116(Mn0.74Mn0.093 □ 0.167)O1.7.OH0.3
Y (mm)
X (mm)

a) b) c) d)

Fig. 4